Unraveling the molecular conformations of a single ruthenium complex adsorbed on the Ag(111) surface by calculations

Youness Benjalal, Jacques Bonvoisin, Xavier Bouju

Unraveling the molecular conformations of a single ruthenium complex adsorbed on the Ag(111) surface by calculations

Youness Benjalal,[a] Jacques Bonvoisin [b] and Xavier Bouju *[b]

The tris(dibenzoylmethanato)ruthenium ($Ru(dbm)_3$) molecule has recently been characterized by scanning tunneling microscopy (STM) experiments upon adsorption on Ag(111). The adsorbed $Ru(dbm)_3$ molecule shows two conformations with respect to the $[1\bar{1}0]$ direction of the substrate, one with a three-lobed feature and the other one with a bi-lobed structure. For each of these structures, the molecule can take two geometries (states). Molecular mechanics calculations in a semi-empirical framework and STM calculated images reveal that these states on the substrate originate from the enantiomer of the $Ru(dbm)_3$ molecule in the case of three-lobed structure and from the rotation of the two phenyls in the top dbm moities for the bi-lobed form.

Introduction

For several decades, a field of research has been focusing on the development of molecules capable of mimicking basic electronic devices, namely molecular electronics.[1–3] Among the different components, one of the most emblematic is the molecular switch.[4–28] In short, this corresponds to a molecule exhibiting two states that can be switched back and forth due to an external stimulus. These states reveal generally a conformational change that induces a change in the electronic properties of the molecule. Most of the examples already reported in the literature deal with molecules deposited on a surface and involve single molecules or self-assembled molecules in the form of a thin molecular mono-layer. To characterize the properties of single molecules or a localized area of a two-dimensional molecular layer, the most used techniques are local-probe based methods, and more specifically scanning tunneling microscopy (STM). Not only one can obtain images with a sub-ångström resolution but also with such a fine positioning of the tip one can generate very local stimuli. These stimuli can be light or local electric fields, which are enhanced beneath the tip, tunneling electrons, or a mechanical action provided by the tip.[29–33]

In this work, we describe with numerical methods the adsorption and switching of the tris(dibenzoylmethanato)ruthenium ($Ru(dbm)_3$) molecule on the Ag(111) surface;[34,35] this molecule is of particular interest in the route towards the synthesis of larger entities devoted to charge transfer and logic gates.[36–39] Such a molecule with a Ru core can be considered as a precursor of a mixed-valence complex that is interesting for specific electronic properties through charge transfer generating different oxidation states.[40,41] Generally, these properties are probed with ensemble measurement techniques but STM allows one to address the single molecule level. Indeed, a bias voltage pulse above such a complex can modify these states with the help of the inelastic contribution of the tunneling current.[42–45] Before that, one needs to understand the adsorption and the switching properties of an isolated molecule and this is the purpose of the present work. For that, we have performed molecular mechanics and STM image calculations. We have determined the corresponding rotation and diffusion barriers of an isolated molecule on the Ag(111) surface in the framework of the semi-empirical mono-electronic Hamiltonian of the ASED+ molecular orbital method.[46,47] On the other hand, theoretical calculations of the STM images have been performed with the extended Hückel molecular orbital-elastic scattering quantum chemistry (EHMO-ESQC) code.[48,49] This study reveals that the adsorption of $Ru(dbm)_3$ on Ag(111) results in two adsorption geometries, three-lobed and bi-lobed objects, each one having itself two distinct types of structure. These overall numerical results are in very good agreement with experimental results.[35]

Details

The $Ru(dbm)_3$ molecule in the gas phase is a three-dimensional object containing 85 atoms, consisting of three dibenzoylmethanato (dbm) groups. These groups are planar and each of them is linked to the ruthenium core atom by two oxygen

[a] *Université Sultan Moulay Slimane, Faculté polydisciplinaire, Département de chimie, Béni Mellal, Morocco. E-mail: y.benjalal@usms.ma*
[b] *CEMES-CNRS, Université de Toulouse, Toulouse, France. E-mail: xavier.bouju@cemes.fr*

atoms generating an octahedral structure. The size of the molecule is 1.28 nm between two adjacent dbm and 1.21 nm between opposite hydrogen atoms in each dbm group in the gas phase (Fig. 1).

Once deposited on the Ag(111) surface, the geometry of the molecule changes drastically. The adsorbed structure was examined by using an extended semi-empirical atom superposition and electron delocalization (ASED+) approach.[46,47,50–52] This method is based on the extended Hückel molecular orbital theory and is a powerful numerical tool to describe the behavior of large molecules. This numerical code has already proven its reliability to calculate the adsorption state using various molecular systems on metallic surfaces,[53–56] insulating films,[57] and semiconducting surfaces.[58,59] Moreover, ASED+ results have already shown very good agreement with DFT results.[46,47] Standard parameters for carbon, hydrogen, and oxygen were used.[46,47] The (H_{ii}, ζ) extended Hückel parameters for Ru were chosen as Ru 5s (H_{ii} = 8.60 eV, ζ_1 = 2.078), Ru 5p (H_{ii} = 3.28 eV, ζ_1 = 2.043) and Ru 4d (H_{ii} = 11.12 eV, ζ_1 = 5.378, and ζ_2 = 2.303 with weighting coefficients of 0.534 and 0.6365, respectively), taken from Hoffmann *et al.*[60] These parameters have been successfully used for the ruthenium tris(β-diketonato) complexes previously studied.[34,55]

Calculated STM images were obtained within the electron scattering quantum chemistry (ESQC) method.[48,49] This method describes the electronic scattering between the substrate and the tip by modeling the chemical structure of the tunnel gap (substrate, molecule, tip apex, and tip substrate). The algorithm determines the electronic coupling of atoms in the tunnel junction with a mono-electronic Hamiltonian at the semi-empirically extended Hückel molecular orbital (EHMO) level. From the scattering matrix of the STM junction, the tunnel current is evaluated by using the Landauer formula. The realistic geometry of all the components composing the STM junction is explicitly considered with a full atomic representation including the tip itself and a set of atomic orbitals is associated with each atomic site. ESQC is reliable to provide accurate STM images not only for small systems but also for large adsorbed molecules.[34,54–56,61–64]

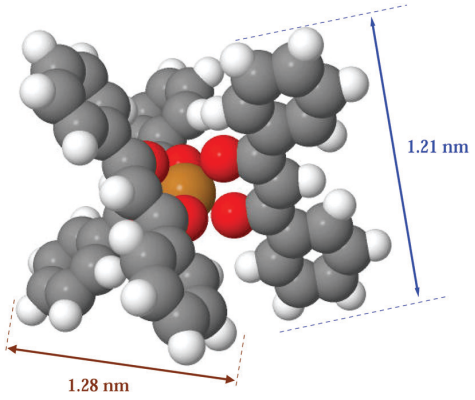

Fig. 1 Optimized chemical structure of a tris(dibenzoylmethanato)ruthenium ($Ru(dbm)_3$) molecule in the gas phase (carbon atoms are in gray, hydrogen in white, oxygen in red and the central brown atom is ruthenium).

Results and discussion

The relaxed adsorption position of the $Ru(dbm)_3$ molecule on the Ag(111) surface is identified with ASED+. This gives two adsorption structures.

Tri-lobed geometry

In the first one called the T geometry (Fig. 2), the molecule lies on the Ag(111) surface with three phenyl groups in contact with the surface keeping an octahedral geometry with the oxygen atoms. The molecular geometry is shown in Fig. 2(b) where all the atoms closest to the surface are at a height of ∼2.5 Å. The adsorption energy including the van der Waals interaction between the molecule and the metallic surface reaches 0.34 eV. The corresponding STM images of a $Ru(dbm)_3$ molecule calculated with ESQC with parameters (bias voltage and tunneling current threshold for constant-current imaging mode) similar to those used in experiments[35] show a three-lobe structure (Fig. 3). ASED+ investigations have been performed in order to calculate the rotation barrier when the molecule lies on the different adsorption sites, that is to say when the Ru central atom is above top, bridge and hollow sites. These calculations are presented in Fig. 2(a). The curves describe the adsorption energy variation for the three sites by considering a molecule with all the degrees of freedom free to

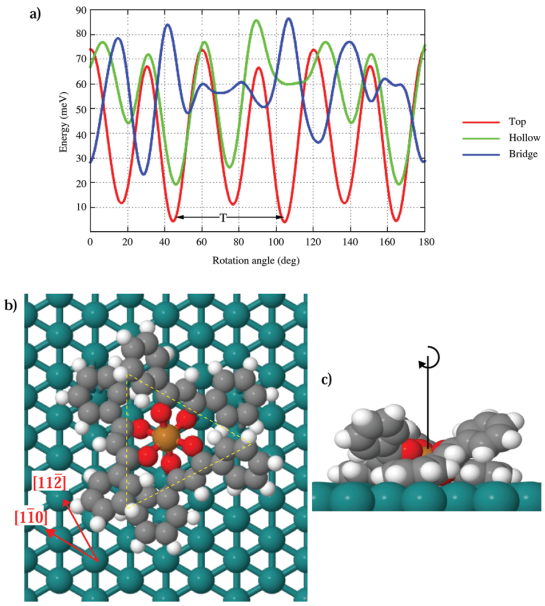

Fig. 2 (a) Variation of the rotation barriers of an adsorbed $Ru(dbm)_3$ molecule when the central Ru atom is above a top (red), hollow (green), and bridge (blue) site of the Ag(111) surface (tri-lobed structure). The curves show the adsorption energy during the rotation taking into account the relaxation of the molecule at each step. The two minima indicated with black arrows are separated by 60° and correspond to the symmetry of the molecule on the surface. Top view (b) and side view (c) of the calculated model of $Ru(dbm)_3$ above a top site on Ag(111) deduced from ASED+ optimization. Carbon atoms are in gray, hydrogen in white, oxygen in red, the central brown atom is ruthenium and Ag atoms are in blue. The red arrows indicate the [1$\bar{1}$0] and [11$\bar{2}$] directions of the surface.

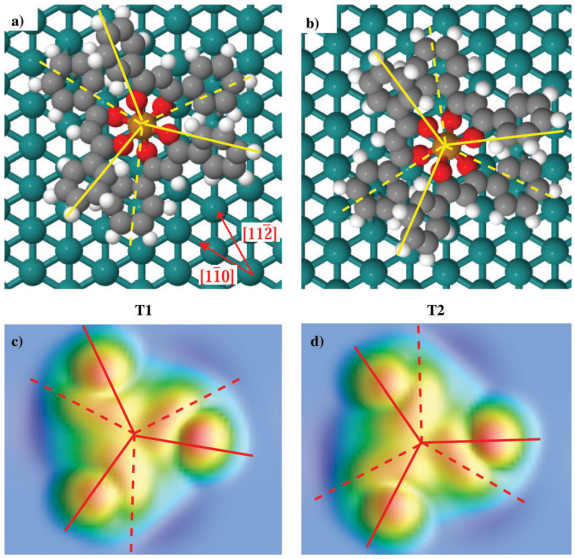

Fig. 3 (a and b) Calculated models of a $Ru(dbm)_3$ molecule adsorbed on Ag(111) (structures T_1 and T_2). Full (dashed) yellow lines identify the Ru atom-upward (downward) phenyl directions of the three dbm groups. (c and d) EHMO-ESQC calculated images of a $Ru(dbm)_3$ molecule adsorbed on Ag(111) as shown in (a and b) respectively, under the same tunneling conditions as in the experimental STM.

relax except the x and y coordinates of the central reference atom and of the oxygen atoms, which are kept frozen. The three energy curves give a relatively fair estimation of the rotation barrier along the [111] direction, which is perpendicular to the substrate (Fig. 2(c)), according to the surface site on which the center of the molecule is located. It can be observed that the top site is the most stable and that the differences relative to the hollow and bridge sites are $\sim$15 and $\sim$20 meV, respectively. Whatever the adsorption site considered, the rotation barrier can be calculated and this yields periodic curves with a periodicity of 60° related to the symmetry of the molecule and the surface. The cross-over points of the three curves are indicative of a barrier which reflects a combination of translation and rotation allowing diffusion on the surface. Moreover, the presented ASED+ calculation does not include the presence of the tip nor the local electrostatic field; these terms probably do not break the apparent symmetry of the energy barriers of rotation due to the large tip–surface distance in the imaging mode and the low bias voltage, so that the molecule stays in the main top site.

Furthermore, the structure presented in Fig. 2 suggests the existence of a chiral property. Indeed, the adsorption process generates two enantiomers for the T geometry on the Ag(111) surface (enantiomers T_1 and T_2) as indicated in Fig. 3(a and b). In the T_2 geometry, there is an inversion of the position of the phenyl groups with respect to T_1: the three phenyls in contact with the surface in T_1 will be detached in T_2 with a 3D configuration, and *vice versa*. These two geometries have the same energetic characteristics (energy and site of adsorption, rotation and diffusion barrier…) and the same curves found in Fig. 2(a).

Using these enantiomer conformations, STM images were computed with the ESQC technique under the same tunneling conditions as in experiments (Fig. 3(c and d)). In both cases, the three bright lobes in the triangular arrangement correspond to tunneling through the three phenyl groups at the top, while the triangular sub-protrusions are attributed to the three phenyl groups in contact with the surface, which are connected to the center of the molecule *via* the oxygen atoms.

These results given in Fig. 3 are qualitatively consistent with the experimental results and quantitatively reflect the main features presented in ref. 35 demonstrating the chirality of the molecule with its enantiomers on the substrate.

Bi-lobed geometry

The second structure is a bi-lobed structure, called the B geometry. Actually, as observed experimentally,[35] 80% of the molecules present a bi-lobed shape on the surface after evaporation of $Ru(dbm)_3$ on Ag(111).

After relaxation with ASED+, the molecule adopts a conformation with two dbm groups almost parallel to the surface and the third one perpendicular to the surface plane. The geometry is thus formed by a square base with a top molecular part which is along the [1$\bar{1}$0] direction of the surface (Fig. 4(b)). This peculiar geometry is called B_1. The adsorption energy was found to be 0.60 eV where all the atoms closest to the surface are at a height of $\sim$2.5 Å.

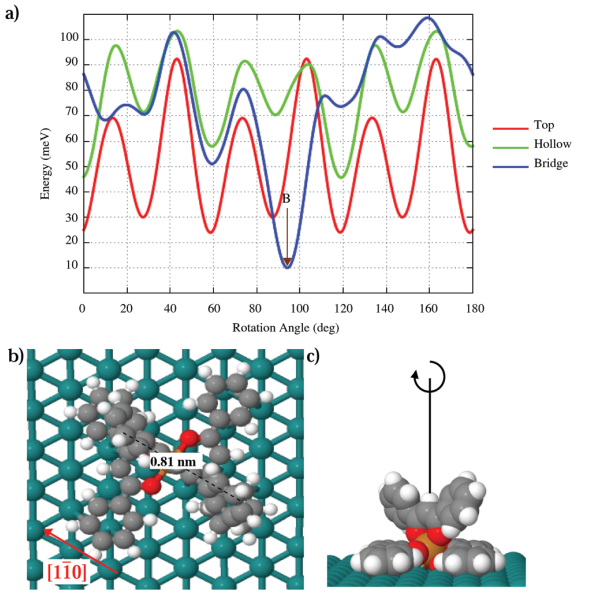

Fig. 4 (a) Calculated rotation energy of a $Ru(dbm)_3$ molecule above a top (red), hollow (green), and bridge (blue) site of the Ag(111) surface (bi-lobed structure). The curves show the adsorption energy during the rotation taking into account the relaxation of the molecule at each step. The red arrow indicates the [1$\bar{1}$0] direction of the surface, with the long axis of the dbm top oriented along this direction [1$\bar{1}$0]. (b) Top view and (c) side view of the calculated adsorption geometry of $Ru(dbm)_3$ on the Ag(111) substrate with the B geometry.

A second geometry is also observed by STM, called B_2. In this case, the top bi-lobed structure has rotated by about 30° with respect to the B_1 case and appears to be oriented along the side of the square base instead of along the diagonal. It should be noted that the general shape of these two forms does not change during the STM experiments[35] since the molecules are not destroyed during evaporation nor modified while scanning.

To understand the origin of the B_1 and B_2 structures, in connection with the intramolecular and molecule–substrate interactions, we calculated the equilibrium structure of $Ru(dbm)_3$ in the bi-lobed structure as a function of the rotational angle of the two phenyls around the C–phenyl bond for the top dbm (Fig. 5).[11] The rotation of the right phenyl is clockwise and it is counterclockwise for the left phenyl around the angle φ and θ, respectively (Fig. 5).[65]

We consider the molecule with two dbm groups parallel to the surface plane such that the central octahedral structure is preserved. To study the π–π intramolecular interactions between the two phenyls of the top dbm group and the other part of the molecule, we calculated the energy variation associated with the rotation of the two phenyls in the top dbm, as shown in Fig. 6. These calculations show the strong π–π repulsion when the molecule is found in the B' position (*i.e.* $\varphi = \theta = \pm 90°$), whereas a minimum energy is observed for $\varphi = \theta = \pm 30°$. A small energy barrier exists for $\varphi = \theta = 0°$ (the B″ case) due to the weak steric crowding between the hydrogen atoms on the top and the H···O interactions on the bottom in this configuration. Consequently, the B_1 ($\varphi = \theta = 30°$) and B_2 ($\varphi = \theta = -30°$) structures correspond to the two minima. Notice that the angle between the two phenyl groups is thus 60°, which is a result in very good agreement with *ab initio* results for the biphenyl molecule.[65]

Experimentally, STM images of the B geometry show two forms, each one with two protrusions.[35] The two lines joining these protrusions form an angle of 30°. STM image calculations of forms B_1 and B_2 obtained by ASED+ relaxation [Fig. 7(a and c)] exhibit similar features [Fig. 7(b and d)]. Moreover, the angle between the two orientations is also about 30°. The agreement is thus excellent. This indicates that the rotation of about 30° of the bi-lobed forms in the experimental and calculated STM images (Fig. 7(b and d)) can be explained by the rotation of each phenyl in the top dbm group by 60° for B_1 and −60° for B_2 around the C–phenyl bond as indicated in Fig. 6(b).

The calculations of the STM images in both the B_1 and B_2 cases in Fig. 7(b and d) show that the two bright lobes in the linear arrangement correspond to the two phenyl groups in the top dbm group, which is oriented along the direction [1$\bar{1}$0], with an apparent height of about 3.9 Å. The two protrusions are separated by about 8.7 Å; this value is in good agreement with the distance between two opposite phenyl groups in the top dbm group of the bi-lobed structure, which is about 8.1 Å (Fig. 4(b) and 5). It is now well-known that reversible switching between two molecular states can be induced by an STM tip. A change in the potential energy surface with respect to particular degrees of freedom may result in a modification of an energy barrier between two states. This change can be generated by the presence of the tip at a relatively low tip–surface distance, *e.g.* by creating a van der Waals trap,[61] or by an extra induction energy provided by the electric field in the STM junction.[11,16] Here, a switch between the two states has been observed when the tip is located above one of the molecule lobes, as discussed previously.[35] This $B_1 \leftrightarrow B_2$ switching effect is compatible with the low energy barrier of 60 meV, as shown in Fig. 6.[12,65] Our theoretical results are thus qualitatively consistent and in good agreement with the experimental results.[34,35]

In addition we have demonstrated that the central cage around the Ru atom is not distorted by the interaction of the molecule with the Ag(111) surface for different geometries (T_1, T_2, B_1, and B_2). The Ru atom keeps its coordination sphere

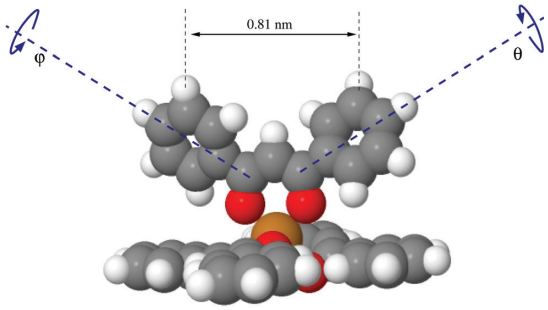

Fig. 5 Model of a $Ru(dbm)_3$ molecule on the Ag(111) substrate obtained by ASED+ calculations (type B) with the rotational angles φ and θ of the two phenyl groups around the C–phenyl bond of the top dbm.

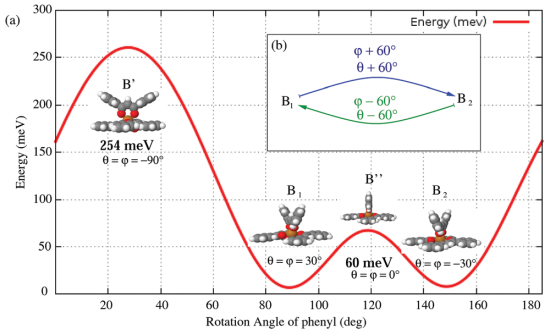

Fig. 6 Energy variation of the $Ru(dbm)_3$ molecule adsorbed on the Ag(111) surface (type B) as a function of the rotational angle of the two phenyl groups around the C–phenyl bonds on the top dbm.

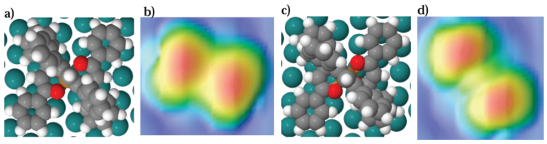

Fig. 7 (a and c) Space-filling model of a $Ru(dbm)_3$ molecule adsorbed on Ag(111) (structures B_1 and B_2, respectively). (b and d) EHMO-ESQC calculated images of a $Ru(dbm)_3$ molecule adsorbed on Ag(111) for the forms B_1 and B_2, respectively, under the same tunneling conditions as in experiments.

intact (the distance between Ru and O atoms is 2.09 ± 0.03 Å), meaning that in this case the complex coordination atom is not influenced by the interaction of the molecule with the surface. Finally, it was experimentally observed that the switching from T to B occurs for a bias voltage around +2.5 V. Further calculations, but out of the scope of the present paper, should be performed to determine the energetic barrier to go from T to B with explicit consideration of the electric field beneath the STM tip and the molecule using a self-consistent procedure,[66] and an accurate dipole moment calculation of the distorted octahedral cage due to adsorption and the Jahn–Teller effect.

Conclusion

In this work, we have shown that the tris(dibenzoylmethanato)-ruthenium molecule adsorbs in two structures on Ag(111) by fully relaxing the molecular structures: a bi-lobed and a three-lobed geometry. For this last one, we have shown that this object presents two orientations related to the geometry of the molecular enantiomers on the surface. These results are in good agreement with experimental results in which the T geometry corresponds to three dbm groups forming an octahedral structure on Ag(111). With the second bi-lobed geometry, we have described and presented the possible reversible switching between two stable states of this complex when adsorbed on Ag(111). The B_1 molecular structure has two dbm groups located almost parallel to the Ag(111) surface forming a square pedestal, while the third dbm group is perpendicular to the substrate plane and is directed along the [1$\bar{1}$0] direction. The other structure B_2 can be deduced from B_1 by a mutual rotation of the top phenyl groups. Molecular mechanics calculations have shown that a small energy barrier exists between these two states, compatible with the switching effect observed experimentally. Additionally, STM image calculations of both structures reveal that each structure shows two protrusions and that their respective orientation with the substrate is in agreement with experimental results. We calculated under the same conditions as the experiment the STM images of these structures, B_1 and B_2. The results show that the bi-lobed shape has rotated by about 30° due to the flexibility of the two phenyl groups in the top dbm. This demonstrates that it is also possible to obtain a B_2 shape on Ag(111) from a B_1 object with the help of a stimulus provided by the STM tip.

Conflicts of interest

There are no conflicts to declare.

Acknowledgements

We thank R. Coratger (CEMES-CNRS) for discussions. This work was supported by Programme Investissements d'Avenir under Program No. ANR-11-IDEX-0002-02, Reference No. ANR-10-LABX-0037-NEXT.

References

1 C. Joachim, J. K. Gimzewski and A. Aviram, *Nature*, 2000, **408**, 541–548.
2 J. C. Cuevas and E. Scheer, *Molecular Electronics: An Introduction to Theory and Experiment*, World Scientific, Singapore, 2010.
3 K. Moth-Poulsen, *Handbook of Single-Molecule Electronics*, CRC Press, Boca Raton, 2016.
4 *Molecular switches*, ed. B. L. Feringa, Wiley-VCH, Weinheim; Chichester, 2001.
5 J. K. Gimzewski and C. Joachim, *Science*, 1999, **283**, 1683–1688.
6 V. J. Langlais, R. R. Schlittler, H. Tang, A. Gourdon, C. Joachim and J. K. Gimzewski, *Phys. Rev. Lett.*, 1999, **83**, 2809–2812.
7 F. Moresco, G. Meyer, K.-H. Rieder, H. Tang, A. Gourdon and C. Joachim, *Phys. Rev. Lett.*, 2001, **86**, 672–675.
8 C.-S. Tsai, J.-K. Wang, R. T. Skodje and J.-C. Lin, *J. Am. Chem. Soc.*, 2005, **127**, 10788–10789.
9 N. Katsonis, T. Kudernac, M. Walko, S. J. van der Molen, B. J. van Wees and B. L. Feringa, *Adv. Mater.*, 2006, **18**, 1397–1400.
10 G. Füchsel, T. Klamroth, J. Dokić and P. Saalfrank, *J. Phys. Chem. B*, 2006, **110**, 16337–16345.
11 M. Alemani, M. V. Peters, S. Hecht, K.-H. Rieder, F. Moresco and L. Grill, *J. Am. Chem. Soc.*, 2006, **128**, 14446–14447.
12 B.-Y. Choi, S.-J. Kahng, S. Kim, H. Kim, H. Kim, Y. Song, J. Ihm and Y. Kuk, *Phys. Rev. Lett.*, 2006, **96**, 156105.
13 J. Henzl, M. Mehlhorn, H. Gawronski, K.-H. Rieder and K. Morgenstern, *Angew. Chem., Int. Ed.*, 2006, **45**, 603–606.
14 P. Liljeroth, J. Repp and G. Meyer, *Science*, 2007, **317**, 1203–1206.
15 G. Pace, V. Ferri, C. Grave, M. Elbing, C. von Hanisch, M. Zharnikov, M. Mayor, M. A. Rampi and P. Samori, *Proc. Natl. Acad. Sci. U. S. A.*, 2007, **104**, 9937–9942.
16 M. Comstock, N. Levy, A. Kirakosian, J. Cho, F. Lauterwasser, J. Harvey, D. Strubbe, J. Fréchet, D. Trauner, S. Louie and M. Crommie, *Phys. Rev. Lett.*, 2007, **99**, 038301.
17 M. Alemani, S. Selvanathan, F. Ample, M. V. Peters, K.-H. Rieder, F. Moresco, C. Joachim, S. Hecht and L. Grill, *J. Phys. Chem. C*, 2008, **112**, 10509–10514.
18 C. Dri, M. V. Peters, J. Schwarz, S. Hecht and L. Grill, *Nat. Nanotechnol.*, 2008, **3**, 649–653.
19 N. Henningsen, R. Rurali, K. J. Franke, I. Fernández-Torrente and J. I. Pascual, *Appl. Phys. A: Mater. Sci. Process.*, 2008, **93**, 241–246.
20 J. Henzl and K. Morgenstern, *Phys. Chem. Chem. Phys.*, 2010, **12**, 6035–6044.
21 A. Safiei, J. Henzl and K. Morgenstern, *Phys. Rev. Lett.*, 2010, **104**, 216102.
22 T. Leoni, O. Guillermet, H. Walch, V. Langlais, A. Scheuermann, J. Bonvoisin and S. Gauthier, *Phys. Rev. Lett.*, 2011, **106**, 216103.
23 K. Ariga, T. Mori and J. P. Hill, *Soft Matter*, 2012, **8**, 15–20.
24 W. Auwarter, K. Seufert, F. Bischoff, D. Ecija, S. Vijayaraghavan, S. Joshi, F. Klappenberger, N. Samudrala and J. V. Barth, *Nat. Nanotechnol.*, 2012, **7**, 41–46.
25 U. Jung, C. Schütt, O. Filinova, J. Kubitschke, R. Herges and O. Magnussen, *J. Phys. Chem. C*, 2012, **116**, 25943–25948.

26 E. Kazuma, M. Han, J. Jung, J. Oh, T. Seki and Y. Kim, *J. Phys. Chem. Lett.*, 2015, **6**, 4239–4243.
27 K. Scheil, T. G. Gopakumar, J. Bahrenburg, F. Temps, R. J. Maurer, K. Reuter and R. Berndt, *J. Phys. Chem. Lett.*, 2016, 2080–2084.
28 S. Jaekel, A. Richter, R. Lindner, R. Bechstein, C. Nacci, S. Hecht, A. Kühnle and L. Grill, *ACS Nano*, 2018, **12**, 1821–1828.
29 S. Gauthier, *Appl. Surf. Sci.*, 2000, **164**, 84–90.
30 F. Moresco, *Phys. Rep.*, 2004, **399**, 175–225.
31 R. Otero, F. Rosei and F. Besenbacher, *Annu. Rev. Phys. Chem.*, 2006, **57**, 497–525.
32 S.-W. Hla, *Jpn. J. Appl. Phys.*, 2008, **47**, 6063–6069.
33 Q. Sun and W. Xu, *ChemPhysChem*, 2014, **15**, 2657–2663.
34 S. Munery, N. Ratel-Ramond, Y. Benjalal, L. Vernisse, O. Guillermet, X. Bouju, R. Coratger and J. Bonvoisin, *Eur. J. Inorg. Chem.*, 2011, 2698–2705.
35 L. Vernisse, O. Guillermet, J. Bonvoisin and R. Coratger, *Surf. Sci.*, 2014, **619**, 98–104.
36 F. Jäckel, U. Perera, V. Iancu, K.-F. Braun, N. Koch, J. Rabe and S.-W. Hla, *Phys. Rev. Lett.*, 2008, **100**, 126102.
37 H. Walch, T. Leoni, O. Guillermet, V. Langlais, A. Scheuermann, J. Bonvoisin and S. Gauthier, *Phys. Rev. B: Condens. Matter Mater. Phys.*, 2012, **86**, 075423.
38 J. Bonvoisin and I. Ciofini, *Dalton Trans.*, 2013, **42**, 7943–7951.
39 M. Hliwa, J. Bonvoisin and C. Joachim, *Architecture and Design of Molecule Logic Gates and Atom Circuits*, Springer Berlin Heidelberg, 2013, pp. 237–247.
40 S. Guo and S. A. Kandel, *J. Phys. Chem. Lett.*, 2010, **1**, 420–424.
41 A. Schramm, C. Stroh, K. Dössel, M. Lukas, O. Fuhr, H. v. Löhneysen and M. Mayor, *Chem. Commun.*, 2013, **49**, 1076–1078.
42 W. Ho, *J. Chem. Phys.*, 2002, **117**, 11033–11061.
43 K. Morgenstern, *Prog. Surf. Sci.*, 2011, **86**, 115–161.
44 Y. Kim, K. Motobayashi, T. Frederiksen, H. Ueba and M. Kawai, *Prog. Surf. Sci.*, 2015, **90**, 85–143.
45 M. Ternes, *Prog. Surf. Sci.*, 2017, **92**, 83–115.
46 F. Ample and C. Joachim, *Surf. Sci.*, 2006, **600**, 3243–3251.
47 F. Ample and C. Joachim, *Surf. Sci.*, 2008, **602**, 1563–1571.
48 P. Sautet and C. Joachim, *Phys. Rev. B: Condens. Matter Mater. Phys.*, 1988, **38**, 12238–12247.
49 P. Sautet and C. Joachim, *Chem. Phys. Lett.*, 1991, **185**, 23–30.
50 A. B. Anderson, *Int. J. Quantum Chem.*, 1994, **49**, 581–589.
51 G. Calzaferri, L. Forss and I. Kamber, *J. Phys. Chem.*, 1989, **93**, 5366–5371.
52 M. Bosson, C. Richard, A. Plet, S. Grudinin and S. Redon, *J. Comput. Chem.*, 2012, **33**, 779–790.
53 U. G. E. Perera, F. Ample, H. Kersell, Y. Zhang, G. Vives, J. Echeverria, M. Grisolia, G. Rapenne, C. Joachim and S. W. Hla, *Nat. Nanotechnol.*, 2013, **8**, 46–51.
54 C. J. Villagomez, O. Guillermet, S. Goudeau, F. Ample, H. Xu, C. Coudret, X. Bouju, T. Zambelli and S. Gauthier, *J. Chem. Phys.*, 2010, **132**, 074705.
55 L. Vernisse, S. Munery, N. Ratel-Ramond, Y. Benjalal, O. Guillermet, X. Bouju, R. Coratger and J. Bonvoisin, *J. Phys. Chem. C*, 2012, **116**, 13715–13721.
56 C. J. Villagómez, F. Castanié, C. Momblona, S. Gauthier, T. Zambelli and X. Bouju, *Phys. Chem. Chem. Phys.*, 2016, **18**, 27521–27528.
57 C. Bombis, F. Ample, J. Mielke, M. Mannsberger, C. J. Villagómez, C. Roth, C. Joachim and L. Grill, *Phys. Rev. Lett.*, 2010, **104**, 185502.
58 Y. Makoudi, E. Duverger, M. Arab, F. Chérioux, F. Ample, G. Rapenne, X. Bouju and F. Palmino, *ChemPhysChem*, 2008, **9**, 1437–1441.
59 X. Bouju, F. Chérioux, S. Coget, G. Rapenne and F. Palmino, *Nanoscale*, 2013, **5**, 7005–7010.
60 K. A. Joergensen and R. Hoffmann, *J. Am. Chem. Soc.*, 1986, **108**, 1867–1876.
61 X. Bouju, C. Girard, H. Tang, C. Joachim and L. Pizzagalli, *Phys. Rev. B: Condens. Matter Mater. Phys.*, 1997, **55**, 16498–16506.
62 M. Yu, N. Kalashnyk, R. Barattin, Y. Benjalal, M. Hliwa, X. Bouju, A. Gourdon, C. Joachim, E. Lægsgaard, F. Besenbacher and T. R. Linderoth, *Chem. Commun.*, 2010, **46**, 5545–5547.
63 Y. J. Dappe, M. Andersen, R. Balog, L. Hornekær and X. Bouju, *Phys. Rev. B: Condens. Matter Mater. Phys.*, 2015, **91**, 045427.
64 M. Yu, Y. Benjalal, C. Chen, N. Kalashnyk, W. Xu, R. Barattin, S. Nagarajan, E. Lægsgaard, I. Stensgaard, M. Hliwa, A. Gourdon, F. Besenbacher, X. Bouju and T. R. Linderoth, *Chem. Commun.*, 2018, **54**, 8845–8848.
65 J. Almlöf, *Chem. Phys.*, 1974, **6**, 135–139.
66 X. Bouju, M. Devel and C. Girard, *Appl. Phys. A: Mater. Sci. Process.*, 1998, **66**, S749–S752.